Additive Manufacturing Letters 11 (2024) 100250

Contents lists available at ScienceDirect

Additive Manufacturing Letters

journal homepage: www.elsevier.com/locate/addlet

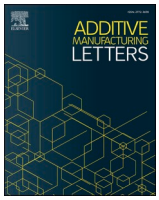

Short Communication

Drop-on-demand 3D printing of programable magnetic composites for soft robotics

Anil Bastola [a,b,*], Luke Parry [a], Robyn Worsley [a], Nisar Ahmed [a], Edward Lester [c], Richard Hague [a], Christopher Tuck [a,*]

[a] Centre for Additive Manufacturing, Faculty of Engineering, University of Nottingham, Nottingham, NG7 2RD, United Kingdom
[b] Mechanical Engineering, Faculty of Science and Engineering, Swansea University, Swansea, SA1 8EN, United Kingdom
[c] Advanced Materials Research Group, Faculty of Engineering, University of Nottingham, Nottingham, NG7 2RD, United Kingdom

ARTICLE INFO

Keywords:
Magnetic composites
Smart materials
Additive manufacturing
3D printing
High-viscosity jetting
Soft robotics

ABSTRACT

Soft robotics have become increasingly popular as a versatile alternative to traditional robotics. Magnetic composite materials, which respond to external magnetic fields, have attracted significant interest in this field due to their programmable two-way actuation and shape-morphing capabilities. Additive manufacturing (AM)/3D printing allows for the incorporation of different functional composite materials to create active components for soft robotics. However, current AM methods have limitations, especially when it comes to printing smart composite materials with high functional material content. This is a key requirement for enhancing responsiveness to external stimuli. Commonly used AM methods for smart magnetic composites, such as direct ink writing (DIW), confront challenges in achieving discontinuous printing, and enabling multi-material control at the voxel level, while some AM techniques are not suitable for producing composite materials. To address these limitations, we employed high-viscosity drop-on-demand (DoD) jetting and developed programmable magnetic composites filled with micron-sized hard magnetic particles. This method bridges the gap between conventional ink-jetting and DIW, which require printing inks with viscosities at opposite ends of the spectrum. This high-viscosity DoD jetting enables continuous, discontinuous, and non-contact printing, making it a versatile and effective method for 3D printing functional magnetic composites even with micron-sized fillers. Furthermore, we demonstrated stable magnetic domain programming and two-way shape-morphing actuations of printed structures for soft robotics. In summary, our work highlights high-viscosity DoD jetting as a promising method for printing functional magnetic composites and other similar materials for a wide range of applications.

1. Introduction

Magnetic composite materials are showing increasing potential within several applications, from biomedical engineering to soft robotics [1–7], which consist of magnetic fillers loaded into a non-magnetic matrix, where the benefit of both non-magnetic matrices and magnetic fillers can be harnessed simultaneously. The ability to respond to magnetic fields is particularly interesting, as it opens up the possibility for remote control of devices without the need for direct contact and furthermore offers a quick response [1,7,8]. One type of magnetic material that has attracted significant interest is ferromagnetic composite materials, which offer a higher magnetic response as well as two-way actuation and are therefore useful for a wide range of applications [7–10].

Amongst the ferromagnetic materials available, micron-sized hard magnetic neodymium iron boron ($Nd_2Fe_{14}B$) particles are attractive because of their superior magnetic properties (high coercive field: 750–2000 kA/m [11]) and (re) programmability offered by the wide magnetic hysteresis loop. NdFeB has potential within several fields, including magnetic refrigeration [12], permanent electric motors [13], and soft robotics [5,7,14–17], among others.

The field of soft robotics has emerged as an alternative to traditional robotics, offering flexibility and adaptability for complex tasks. Soft robotics deals with the design, fabrication, and control of robots/actuators made from soft, flexible and active materials. Soft robots have several advantages over traditional rigid robots, including safety, adaptability, energy efficiency, biomimicry etc. with potential applications including but not limited to biomedical and space exploration

* Corresponding authors.
E-mail addresses: a.k.bastola@swansea.ac.uk (A. Bastola), Christopher.Tuck@nottingham.ac.uk (C. Tuck).

https://doi.org/10.1016/j.addlet.2024.100250
Received 12 July 2024; Received in revised form 8 October 2024; Accepted 23 October 2024
Available online 28 October 2024

[18]. Magnetic field-responsive materials offer the potential to enable two-way actuation and precise control of soft robotic components. To unlock the full potential of these magnetic materials, additive manufacturing (AM) techniques have become increasingly applicable, due to the possibility of integration of various materials with diverse properties, enabling the fabrication of complete functional systems [8,14,19–23].

Notable advancements have been made in AM of hard magnetic materials, specifically focusing on the widely recognised example of NdFeB [24]. Current AM techniques to produce NdFeB-based magnetic materials include L-PBF (Laser Powder-Bed Fusion) [25,26], direct energy deposition (DED) [27], selective laser sintering (SLS) [28] binder jetting [29], direct ink writing (DIW) [16,30], and fused filament deposition (FDM) [31]. While certain methods (L-PBF and DED) focus on pure magnetic materials, others such as DIW, FDM, and SLS focus on manufacturing magnetic composite materials, enabling the combined benefit of the matrix material and magnetic fillers with the matrix facilitating the mechanical properties whilst the fillers enabling functional performance.

Current AM methods for magnetic composite materials, such as DIW, the most widely used technique for magnetic composite ink printing [16,30,32–34], primarily focus on the development of materials and structures using contact-based and continuous printing approaches. Such methods encounter inherent challenges when it comes to producing metamaterials, achieving discontinuous printing, and precisely controlling multiple materials at the voxel level. Despite ongoing efforts to overcome these limitations, alternative AM methods such as FDM, SLS and digital light processing (DLP) possess further drawbacks concerning scalability and processability, particularly in terms of achieving magnetic filler loading within the feedstock material, such as filaments (FDM), powders (SLS) and photocurable resins (SLA/DLP).

Material jetting (MJ) is a promising yet largely unexplored method for printing magnetic materials. There are only a few reported instances of jetting soft magnetic materials, including Fe-based, Co-based, and Gd_5Si_4 nanoparticle inks [35–37] and others [38,39]. Drop-on-demand (DoD) ink-jetting offers several advantages, such as non-contact printing, ease of scalability, and printing directly onto the desired substrate of interest. The type and concentration of the filler are important factors in determining the functionality of magnetic composites. Micron-sized magnetic particles (due to better magnetic response) and higher concentrations of the fillers are desired for improved magnetic functionality for magnetic composites. However, the current low-viscosity ink-jetting methods are not capable of depositing composite inks containing micron-sized magnetic particles or higher filler loading. Although recently developed print heads, such as those from Xaar [40] and Quantica [41], have claimed to handling high-viscosity fluids, offering the ability to work at higher filler loadings, and potentially enabling the utilisation of micron-sized particles. Nonetheless, the implementation of DoD AM to fabricate functional magnetic composite materials (or similar composite materials) remains an unexplored area of research, particularly due to the increased viscosity associated with these filler-based inks (up to 70 wt.%) [5].

Printing inks for AM of composite materials typically consist of various components, including monomers/copolymers, crosslinkers, diluents, fillers, surfactants, and other additives. However, incorporating many different components both increases complexity and compromises the main functionality, such as magnetic response. Using currently established ink-jetting methods (requiring low viscosity 5–100 mPa·s inks and Newtonian fluids), it is not yet viable to process micron-sized filler particles, while nanofillers require surface modification, such as ligand attachment, to develop inks which are stable during jetting and are typically of low filler loadings. Conversely, in the DIW method, substantial addition of rheological modifiers, such as silica nanoparticles, is necessary to achieve shear thinning and thixotropic ink properties, typically having a viscosity in the range of 100 Pa.s. Still there are some exceptional cases in DIW where viscosity is enhanced in-situ during printing/jetting via a magnetic field [42]. Consequently, the medium-range viscosity inks developed in this study are facile to formulate, require a minimal number of components usage (oligomer/monomer and fillers), that span the viscosity gap, and functionality, unobtainable via both DIW and Piezo/MEMS ink jetting techniques. Hence, an alternative or enhanced AM technique is required to enable the printing of viscoelastic non-Newtonian mid-viscosity inks, albeit not as high as those used in DIW.

Herein, we present a study of a facile, yet unexplored route in additively manufactured functional magnetic materials using DoD high-viscosity jetting (Fig. 1). Our work demonstrates, for the first time, the successful DoD printing of photocurable magnetic materials loaded with micron-sized magnetic fillers (45 wt.%), without limitations from thermally curable counterparts found in the literature. Alongside printing, for highlighting the obtained functionality of the proposed methodology for producing highly controlled programable two-way actuation, examples are presented towards the application in soft robotics.

2. Materials and methods

2.1. Materials

Magnetic ink is developed by employing micron-sized hard magnetic Neodymium Iron Boron particles (NdFeB) (MQFP™ 14–12 ($D_{50} = 5$ μm), Magnequench, Germany) as the fillers and FLGR02 resin (Formlab) as the matrix. NdFeB has 910–1020 kA/m magnetic coercivity, and the post-cure FLGR02 matrix has 5.9–6.6 MPa tensile strength and 80–90 Shore A hardness, according to the supplier. A magnetic filler loading of 45 wt.% was utilised, based on jetting and photocurability optimisation experiments.

A fixed amount of resin and magnetic powders were measured and transferred to a vial. The mixing process was carried out using a high-speed mixer (DAC400.1 FVZ, Germany) for 10 min. This mixer, known as the dual asymmetric centrifuge, combines forces in different planes, allowing for rapid and thorough mixing. The resulting ink mixture remained highly stable; nozzle clogging was not observed even when jetted after 24 h without any additional mixing.

2.2. 3D Printing system

The study utilised an in-house jetting system consisting of a PicoPulse jetting valve (Nordson EFD) and a UV curing station. The system has a computer-controlled 3-dimensional Aerotech stage to ensure accurate positioning of the PicoPulse jetting valve with a precision of 5 μm. Nozzles of differing sizes can be utilised and a 100 μm nozzle was used in this study. The PicoPulse jetting valve employs pneumatic and mechanical actions to operate. The magnetic ink is pressurised up to 1 MPa and then directed through a heated fluid path (capable of reaching 100 °C) into the jetting chamber. Within the chamber, a piezoelectrically-driven piston with a ceramic sealing ball oscillates in response to the printing signal (up to 200 Hz), which in turn opens and closes the nozzle, resulting in the ejection of material. The user can manipulate the pulse time (t_p) and the cycle time (t_c) through the digital controller, but the opening and closing speed of the valve is predetermined and not user controllable. Further details of this jetting system can be found in [43–45].

The jetting was performed on glass substrates, where the substrate was treated with isopropanol (IPA) before jetting and samples were peeled off the substrate after printing using a sharp blade.

2.3. Rheology

Ink rheology was studied using a rheometer (Malvern Kinexus, Netherlands) with a parallel plate geometry (40 mm diameter). To study the viscosity, flow tests were conducted at varying shear rates from 0.1 to 100 s^{-1} at four different temperatures (25, 30, 35, and 40 °C).

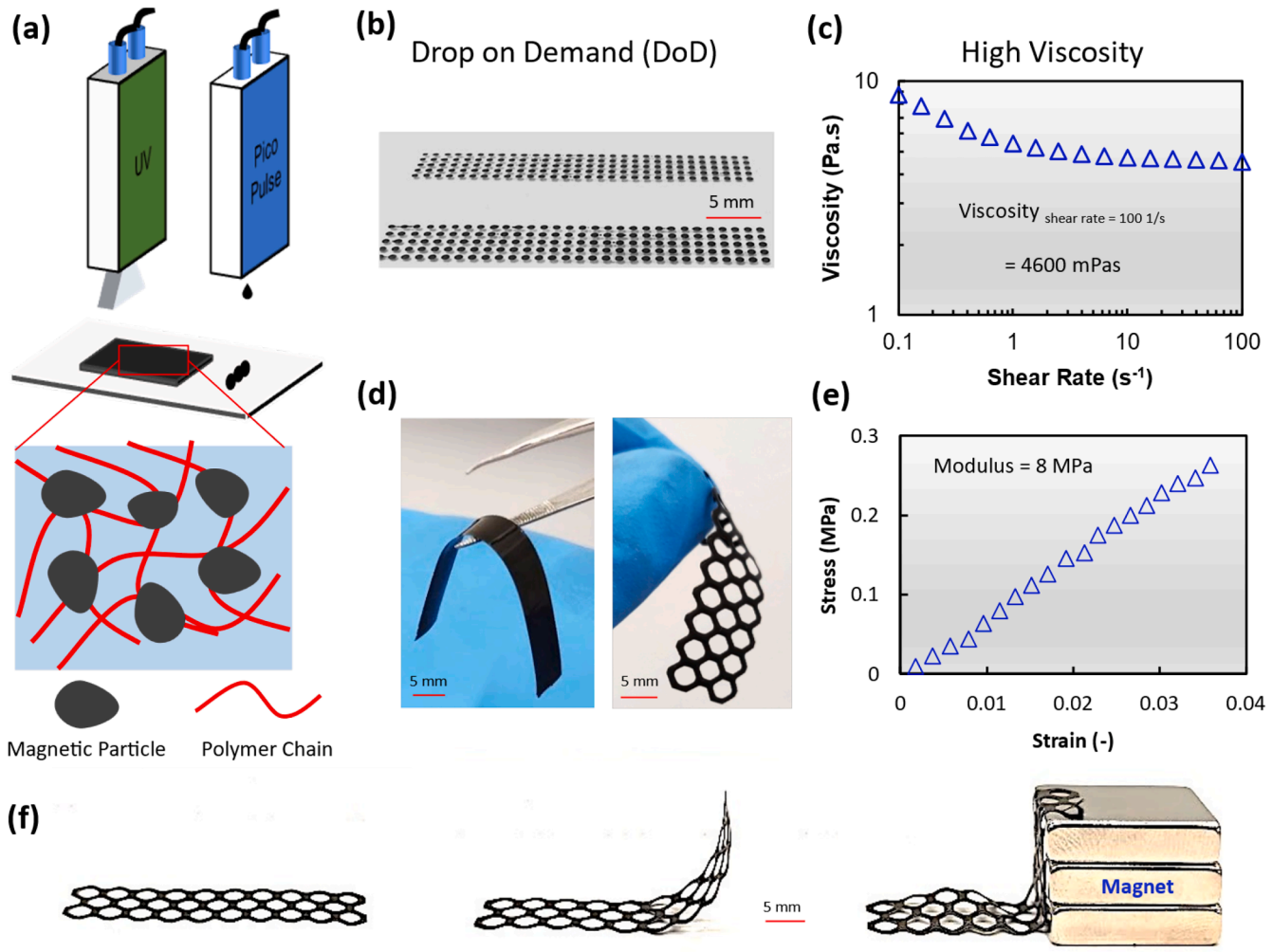

Fig. 1. High viscosity drop-on-demand jetting of flexible magnetic composites. (a) schematics of the jetting process, (b) printed magnetic droplets, (c) ink viscosity, (d) printed flexible magnetic structures, (e) stress-strain response of the printed magnetic materials (f) response of the printed flexible lattice in the presence of a magnetic field.

Viscoelasticity was studied through an amplitude sweep by varying stress levels from 0.1 to 100 Pa at 1 Hz and a frequency sweep by varying frequency from 0.1 to 10 Hz within the linear viscoelastic (LVE) region. Finally, a thixotropy test was conducted to mimic the jetting process and investigate the viscosity recovery of the magnetic ink.

2.4. Magnetic domain programming and actuation

Magnetic programming and actuation were conducted using sets of permanent magnets (20 × 20 × 5 mm N42 Neodymium Magnet, Magnet Expert Ltd, UK) that were stacked together. The magnetic flux density (B) was measured with a magnetometer (Hirst Magnetics GM07, RS pro, UK), and was determined to be 460 mT at the centre of the surface of the three stacked magnets. The magnetic domain programming was verified using a magnetic camera (MagCam, Belgium) by recording small remanence magnetic field of the hard magnetic particles after programming. The MagCam consists of 1000 Hall sensors that measures the change in magnetic flux density providing a 2D magnetic image of the sample with a resolution of 0.1 mm^2. Programming involved placing the samples (typically folded samples to achieve anisotropy) directly on the surface of the stacked magnets for 5 min, while actuation was achieved by bringing the magnet close to the sample and subsequently taking the magnet away from the sample.

3. Results and discussion

Photocurable behaviour and printability were investigated and optimised with varying concentrations of NdFeB fillers incorporated into the matrix. While higher filler loading enhances the magnetic response, it possesses challenges in multi-layer printing due to low photo-absorption and layer delamination. Unlike thermo-curable resins/inks, achieving multi-layer printing using photo-curable resin is a challenge, particularly when micron-sized filler particles are present. Thus, optimising the filler loading was the first step and through initial experimentation, we determined that a loading of 45 wt.% magnetic filler offered an optimal balance between jetting and photo-curability, thereby enabling successful multi-layer printing.

3.1. Ink rheology

The rheological properties of the microparticle-based magnetic ink are given in Fig. 2. The magnetic ink initially exhibits a flowing behaviour when subjected to gravity, but its flow is hindered, leading to a delayed response showing a viscoelastic nature. The rheological measurements further validate the observed physical behaviour of the ink.

The ink carrier (without magnetic particles), behaves as a Newtonian fluid, displaying a relatively high viscosity of 2.8 (± 0.2) Pa.s at a shear rate of 0.1 s^{-1}. On the other hand, the magnetic ink (45 wt.% filler)

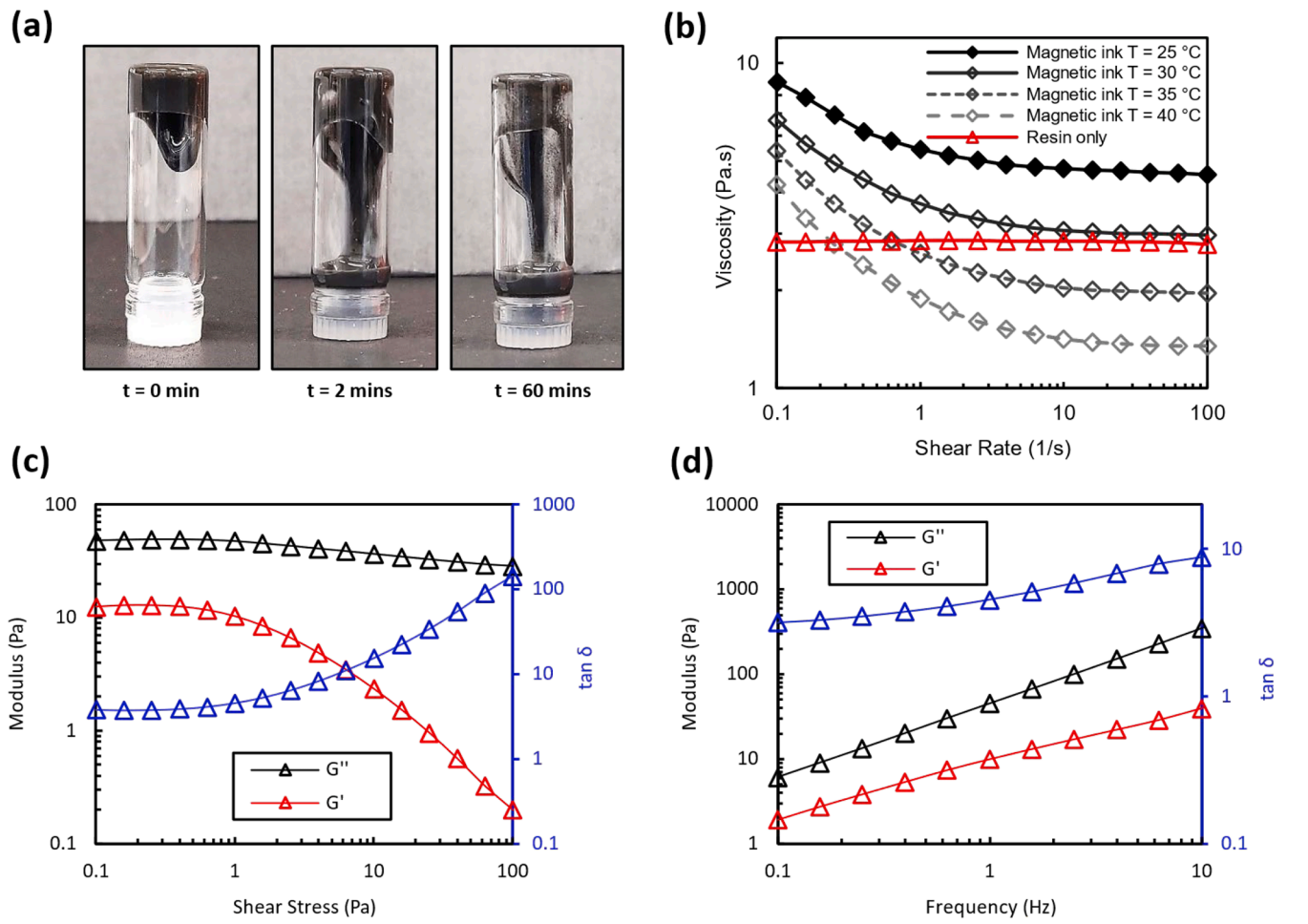

Fig. 2. (a) Photographs of the ink flow under gravity, (b) viscosity as a function of shear rate at various temperatures, (c) viscoelastic behaviour with respect to the amplitude of deformation, and (d) viscoelastic behaviour related to the frequency of deformation, with moduli (G' and G") and loss factor (δ) plotted against shear stress and frequency.

exhibits considerably higher viscosity, measuring 8.7 (± 1.3) Pa.s under the same shear rate. The magnetic ink further demonstrates shear-thinning behaviour, which is more pronounced at the lower shear rates, while at the higher shear rates, the behaviour tends to resemble that of a Newtonian fluid. Additionally, the viscosity of the magnetic ink decreases significantly with increased temperature, surpassing even that of the virgin ink at higher shear rates. For instance, at 40 °C and a shear rate of 0.1 s^{-1}, the viscosity drops to 1.3 Pa.s. Thus, the viscosity of the magnetic ink can be reduced by raising the temperature, increasing the shear rate, or a combination of both during the jetting process.

The viscoelasticity measurements conducted using an amplitude sweep indicate that the ink remains in a fluid phase throughout, as evidenced by the higher value of the loss modulus (G'') compared to the storage modulus (G'). This holds true both within and outside the linear viscoelastic (LVE) region, ensuring the ink maintains a liquid state consistently. The ink demonstrates a weak LVE zone, within the region of shear stress below 1 Pa. Furthermore, it exhibits a stable response to varying deformation frequencies – suggesting that the ink should be stable when jetted at different frequencies. As the rate of deformation increases during the frequency sweep, the damping behaviour of the ink undergoes slight changes, with the loss factor slightly increasing. This behaviour is typical of viscoelastic materials.

3.2. DoD high viscosity jetting

Fig. 3 provides a comprehensive overview of the jetting process and its relationship with ink rheology. The developed ink formulations were jetted using a Nordson PicoPµlse dispensing valve with a 100 µm diameter nozzle. Deposited ink was irradiated layer-wise with an attached UV unit (Phoseon FireEdge FE400 UV LED, 8 W/cm^2 and 395 nm wavelength) for photo-polymerisation, each layer is exposed up to 10 s for photo-polymerisation. Optimal jetting parameters tailored for the magnetic ink are stated in Table 1. The procedure for optimising these print parameters in order to handle materials with diverse viscosities can be found in separate references [44,45].

High-speed imaging was captured for understanding the jetting mechanism. As shown in Fig. 3b, an initial stream of fluid is ejected forming a droplet on the substrate. Upon impact, the fluid stream breaks off causing a recoil back to the nozzle. This recoil phenomenon serves as further evidence of the ink's viscoelastic nature corresponding with findings from the rheological studies. Thus, in high-viscosity jetting, controlled droplets are formed by the break-up of the fluid-stream upon reaching the substrate, unlike discrete droplets encountered in piezo-electric jetting of low-viscosity ink or continuous extrusion of ink with DIW.

As shown in Fig. 3c, it is observed that the droplets spread by wetting the substrate. Initially, the diameter of the jetted droplets ranges from 300 to 350 µm, but eventually, they reach a final equilibrium diameter of 600 to 650 µm. For additional information on the jetting and wetting process, please refer to supplementary video SV1.

Comprehensive rheological studies were undertaken to gain a deeper insight into the jetting process and the subsequent droplet spreading.

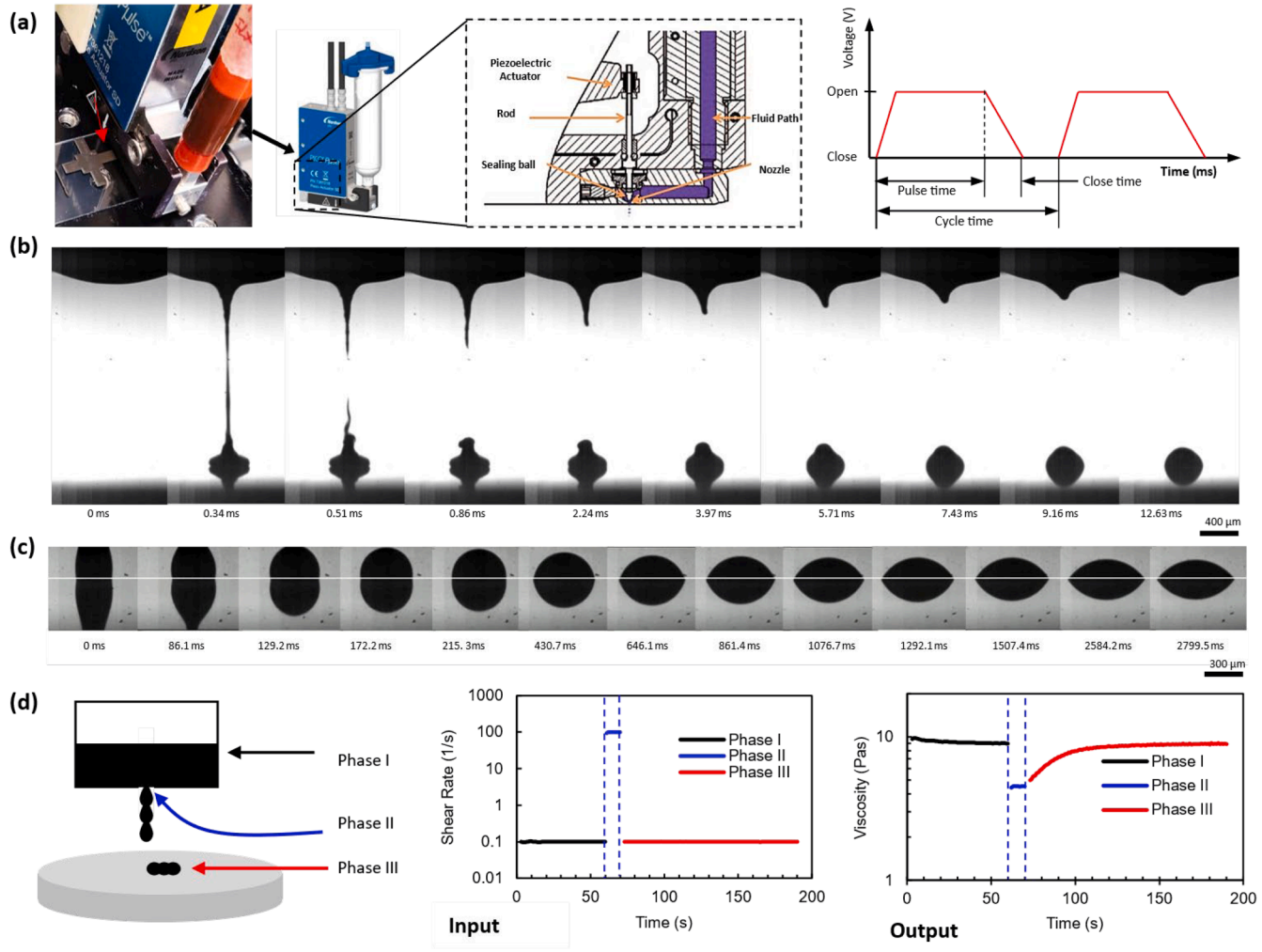

Fig. 3. a) The jetting system showing the Pico valve's key components, typical shape of the jetting waveform illustrated with key parameters: pulse, close, and cycle times. b) High-speed imaging captures of the jetting process. c) Sequence showing the droplet spreading on the substrate after jetting. d) Illustration of the phases of the jetting process and rheological results mimicking the jetting process, showing the recovery of ink viscosity.

Table 1
Optimal print parameters selected for jetting the magnetic ink.

Print Parameter	Pressure	Jetting temperature	Jetting frequency	Drop spacing	Offset height	Pulse time	Close time	Open time
	1 MPa	40 °C	200 Hz	450–500 µm	2 mm	0.3–0.5 ms	0.2 ms	0.25 ms

Viscosity recovery tests provide valuable insight into the jetting process, which can be divided into three distinct phases, as depicted in Fig. 3d. Phase I represents the stable stage within the ink reservoir, while Phase II corresponds to the ejection process, during which the ink is subjected to a high shear rate. Phase III mimics the ink on the print substrate and is of particular significance, as it captures the behaviour of the ink after jetting, including the time taken for the ink to recover its viscosity. To mimic Phase I, a low shear rate of 0.1 s^{-1} was applied on the rheometer for 60 s; although technically zero shear rate would be more appropriate, it is not practically achievable in the experiment. Phase II was simulated by subjecting the ink to a higher shear rate of 100 s^{-1} for 10 s. Finally, the viscosity recovery was examined by reverting to an original shear rate of 0.1 s^{-1} for an additional 120 s.

The viscosity recovery test reveals that the ink takes an extended period to fully recover its viscosity. However, approximately 80 % of its viscosity is regained within a short span of 3–5 s, which aligns closely with observations from the high-speed imaging of the droplet spreading on the substrate. Once the ink reaches an equilibrium state, the droplet's spreading subsides with recovery of 90 % of its initial viscosity. This spreading behaviour (Fig. 3c) can be attributed to the application of high shear force exhibited during jetting, which facilitates the flow of the ink and deformation of the droplet towards an equilibrium state because of shear-thinning (Fig. 2b) until viscosity recovery is attained.

Several factors prevent ink from fully recovering its viscosity. One major factor is viscoelasticity, where inks exhibit both solid-like and fluid-like properties and rheological properties are highly time, frequency, amplitude dependent. Another is shear thinning and thixotropy; thixotropic materials take time to regain their original viscosity after stress is removed, and some may never fully recover due to structural changes. Additionally, mechanical stress and damage play a role. When ink is subjected to high shear force, the polymer network and physical bonds, such as hydrogen and Van der Waals bonds, are broken.

The microparticle magnetic ink remained stable during continuous printing of up to five-hour duration, and when printing was resumed following 24 h. Fig. 4 shows the capabilities, potential, and exemplars of DoD high-viscosity jetting with magnetic materials. Optimal jetting

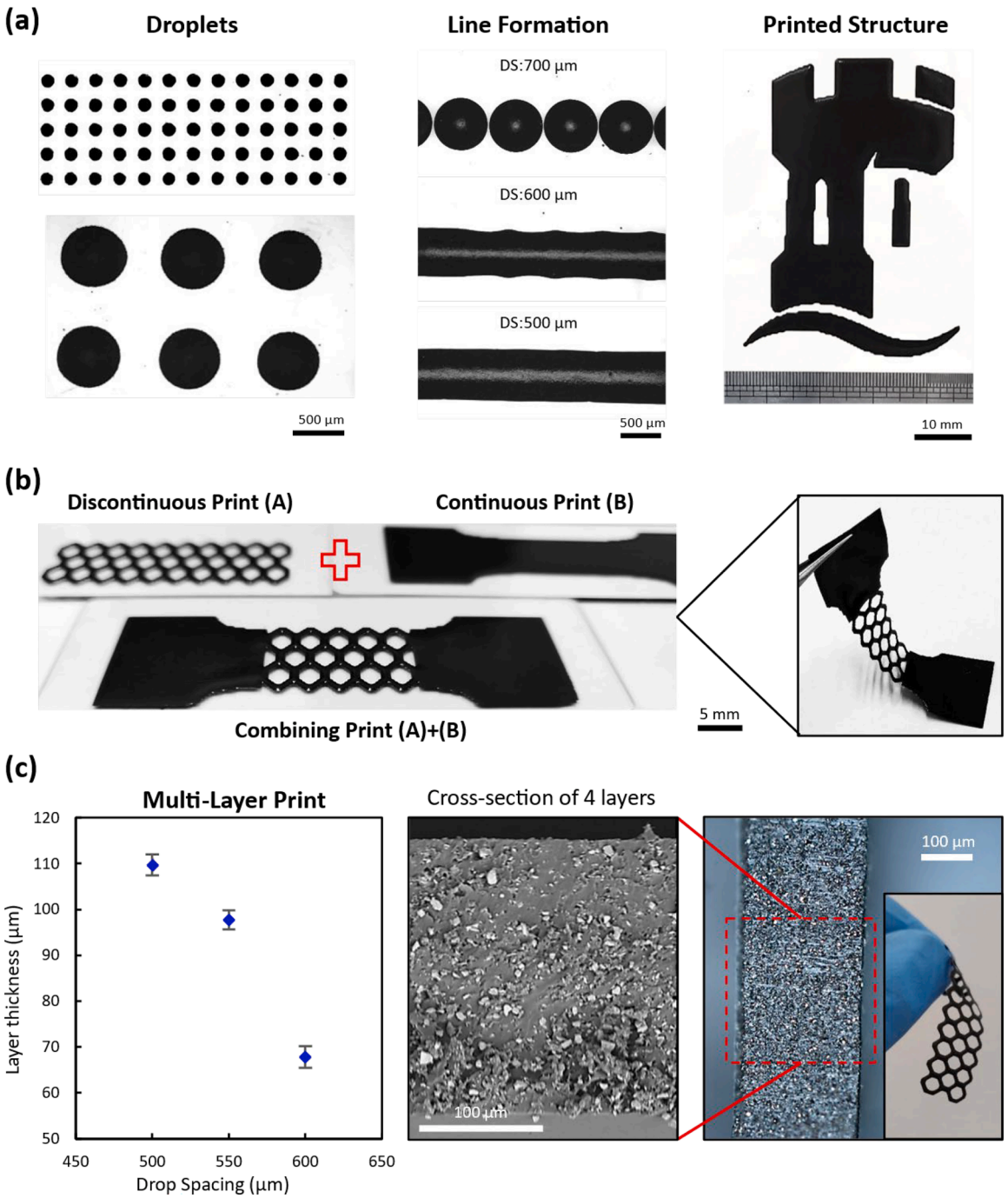

Fig. 4. High viscosity jetted structures. a) Photographs depicting the step-by-step process of creating a magnetic object/structure, beginning with the formation of droplets, followed by droplet merging, subsequent line formation, and finally the formation of the complete structure (University of Nottingham Logo). b) DoD capability to create metamaterial structures, achieved by incorporating both non-continuous and continuous prints within a single structure. c) Multi-layer printing: showing layer thickness and cross-sectional view of the 4-layered printed sample under an optical microscope and SEM. DS stands for drop spacing.

parameters for the ink (Table 1) were selected with the drop spacing varied for control over the layer thickness and crucially special control for feature definition across both (non)-continuous structures obtained. Fig. 4b shows the successful combination of continuous and discontinuous printing, resulting in intricately well-defined structures that are largely unobtainable using extrusion processes such as DIW employed in the production of magnetic composite materials.

The use of photo-curable ink with rapid curing permits simplified extension of deposition in 3D. Thermal or moisture cure systems employed with DIW have tendency for nonconforming 3D structures as material's inability to be self-supporting and proneness to 'sag' due to the extended gelation period encountered with the chemical curing process. Printing of structures in 3D can be applied in various fields such as the development of adjustable stiffness structures or actuators where traditional 2D laminar structures are undesirable. Our focus extends beyond the creation of origami-inspired 2D structures; we demonstrate the capability of magnetic photo-polymerisable ink jetting for continuous printing toward three-dimensional structures.

As with the continuous printing of 2D structures, the drop spacing is further an important parameter in the fabrication of multi-layer (3D) structures, where the pulse time also becomes critical. The preferred parameters for continuous stable printing were determined, with a pulse

time of 0.4 ms and a drop spacing of 600 μm, which correspond to a layer thickness of 65 μm across 3D structures. Cross-sections of the multi-layered samples, as shown in Fig. 4c, confirm the presence of uniform dispersion of NdFeB particles throughout the structure. Although the demonstration involved printing up to four layers, it is important to note that the process can be continued, allowing for the development of structures in the Z-dimension with a relatively high (*c.f.* a typical DIW method) resolution of 65 μm.

The successful printing of intricate structures in a DoD fashion, continuous printing, discontinuous printing, and the production of thin layers and multi-layered structures, showcase this high-viscosity jetting-based AM technique as a promising alternative to DIW in the fabrication of composite materials.

3.3. Functional magnetic structures

To showcase the versatility of the methodology beyond fabrication, we demonstrated the magnetic functionality of the printed structures. For demonstration, two elementary designs were considered: a simple beam and a gripper device with potential applications in soft robotics. For characterisations of the flux-density and the alignment of the magnetic domains in the fabricated material, a magnetic field camera (Magcam) was used.

Printed structures were programmed to impart two-way magnetic functionality by exposing them to a 460 mT magnetic field for 5 min, as depicted in Fig. 5. This programming was effective, as shown by the clear change in magnetic domains in the recorded magnetic images. The unprogrammed printed structure shown in Fig. 5b confirms no orientation of the magnetic domains. Following the programming phase with exposure to an external magnetic field for 5 min, a clear positive out of plane field is exhibited (Fig. 5c).

Flexible beams and grippers were programmed similarly, by folding and exposing them to the same magnetic field. The cross-sectional illustration in Fig. 6 shows the target programmed zone of the samples, depicted using blue and red colouring. This is further supported by magnetic imaging after programming. Typically, an unprogrammed magnetic beam simply deflects or gets attracted to a magnetic field, while a programmed magnetic beam, as shown here, exhibits two-way actuation, confirming the effectiveness of the programming technique along with the magnetic images.

The magnetic actuation of the simple beam (Fig. 6a) is successfully demonstrated through two distinct configurations: the tethered beam and the untethered beam. In the case of the untethered beam, when a magnetic field is applied through its cross-sectional plane, it exhibits two-way movement. Moreover, the untethered beam can execute a flipping action and be easily displaced from its initial location. It is important to note that while the untethered beam is flexible, the magnetic field alone does not alter its shape; rather, it changes its position only by moving within the untethered configuration. On the other hand, the tethered beam not only exhibits two-way deflection but also

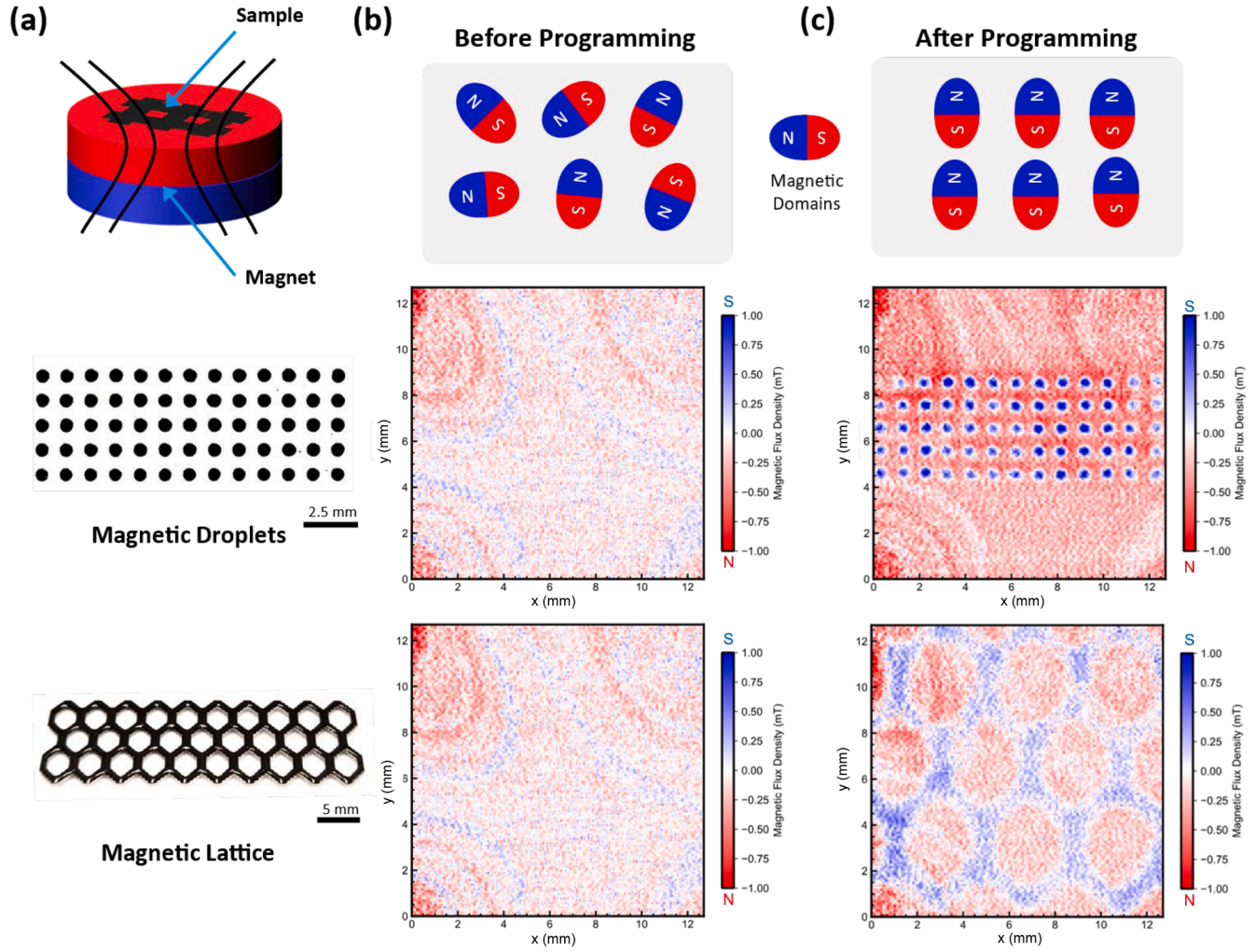

Fig. 5. (a) Process of magnetic domain programming. (b) illustration and results of the magnetic domain of the unprogrammed printed materials and (c) illustration and results of the programmed magnetic materials. Magnetic domains of the samples were recorded using magnetic camera.

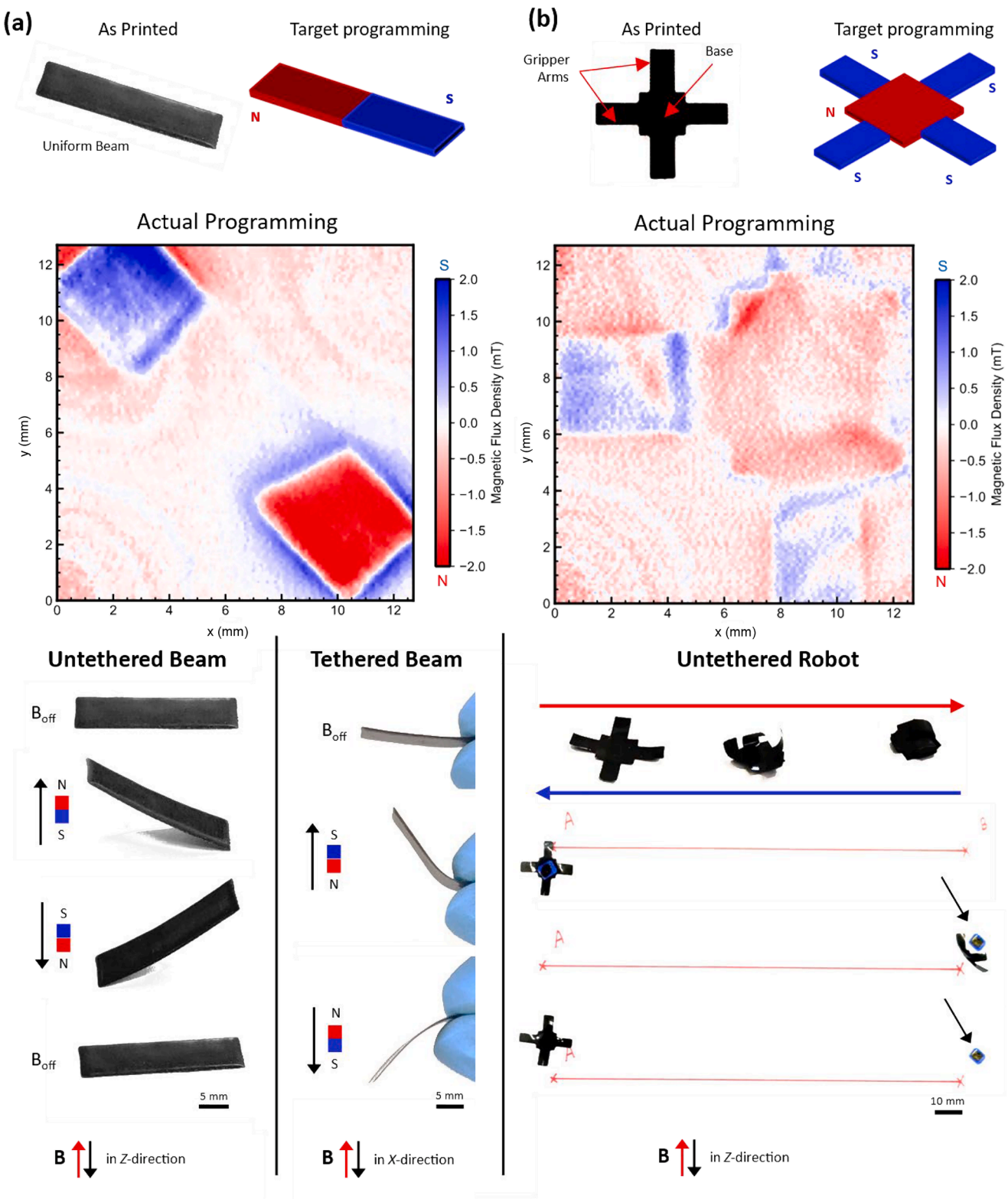

Fig. 6. The demonstration of functionalities of the high viscosity jetted magnetic composite materials. (a) A magnetically programmed beam with bi-directional actuation across both tethered and untethered configurations, and (b) an elementary untethered gripper device that can perform various tasks such as capture, hold, transport, release, and return.

demonstrates shape-morphing capabilities, marked by the bending. Upon the removal of the magnetic field, the tethered beam returns to its original position. These compelling demonstrations highlight the potential of such programmable magnetic structures to serve as magnetic switches or proximity sensors.

The second design shown in Fig. 6b, features a functional robotic gripper with a well-defined structure. It consists of a base designed to securely grasp objects, along with four articulated gripper arms. The programmed gripper possesses the ability to undergo shape transformation when exposed to a magnetic field, offering multi-modality of

functions: capturing objects, their transpiration, deposition, and revert to its original state. Such highly reliable and functional gripper devices could be manufactured at different length scales using high-viscosity jetting. These gripper devices can be incorporated into the body of soft robotics and a magnetic field could be applied through a planar electromagnet directly embedded into the robotic arm.

For a visual demonstration of the magnetic actuation displayed in Fig. 6, please refer to Supplementary Video SV2.

As such, a complete functional magnetic device could be developed as part of a multi-material system using this DoD jetting, where the different components required for magnetic actuation, such as magnetic materials deposited using magnetic ink and electromagnetic coils using conductive ink, can be printed simultaneously.

Although the current investigation focuses on printing single-material magnetic materials, our technique is trivially expandable to multi-material jetting. However, developing structures such as overhangs and latticed-based complex 3D structures is not possible just by using magnetic inks but can be achieved with multi-material jetting when a support ink or other functional ink is jetted simultaneously. These offer the potential fabrication of functionally graded structures. Such structures can be printed by incorporating a range of functional materials such as shape memory materials and electroactive materials, in conjunction with magnetic materials using multi-material jetting. This opens possibilities for diverse applications and further extends the potential of this investigation beyond its current scope.

4. Conclusions

This study demonstrates DoD high-viscosity jetting as an effective means for fabrication of functional magnetic composite materials that overcome the prior limitations of and manufacturing constraints of existing AM methods such as DIW. Crucially, this study showcases its potential for producing intricate structures utilising a microparticle magnetic ink for facilitating the development of responsive 2D and 3D structures and metamaterials. We provide valuable insights into the capabilities of the high-viscosity jetting process through high-speed imaging and subsequent correlations with rheological measurements. The application of high-viscosity jetting offers comparable or even superior capabilities for producing smart composite materials with relatively higher filler loading even with micron-sized fillers. Jetting is trivially extendible to the co-deposition of a broad palette of composites, encompassing elastomeric and polymeric inks, and varying fillers with medium to high filler loading for increased responsiveness.

We not only demonstrated printing capabilities but also demonstrated the functionality of the printed magnetic materials towards soft robotics. It is important to note that in this study, the magnetic actuation of the printed structures was achieved through a secondary programming step, with limited selectivity. Therefore, future work needs to focus on the development of in-situ magnetic domain programming capability during jetting, which would enable selective magnetic domain programming in a single fabrication step. This is smart materials and structures.

Furthermore, high-viscosity jetting enables voxel-wise fabrication of multi-material structures, which could lead to the development of multi-functional and multi-stimuli responsive materials destined across a diverse range of application disciplines.

CRediT authorship contribution statement

Anil Bastola: Writing – review & editing, Writing – original draft, Visualization, Validation, Methodology, Investigation, Formal analysis, Data curation, Conceptualization. **Luke Parry:** Writing – review & editing, Writing – original draft, Visualization, Validation, Methodology, Investigation, Formal analysis, Data curation. **Robyn Worsley:** Writing – review & editing, Writing – original draft, Visualization, Validation, Investigation, Formal analysis. **Nisar Ahmed:** Writing – review & editing, Methodology, Investigation, Data curation. **Edward Lester:** Writing – review & editing, Supervision, Project administration, Funding acquisition, Formal analysis. **Richard Hague:** Writing – review & editing, Supervision, Software, Resources, Project administration, Funding acquisition. **Christopher Tuck:** Writing – review & editing, Writing – original draft, Validation, Supervision, Software, Resources, Project administration, Funding acquisition, Formal analysis.

Declaration of competing interest

The author(s) declared no potential conflicts of interest with respect to the research, authorship, and/or publication of this article.

Acknowledgements

This work was supported by an EPSRC Prosperity Partnership (No. EP/S03661X/1). Authors are grateful to Professor Nicola Morley (University of Sheffield) for providing the magnetic camera (MagCam) to obtain the magnetic images of the samples.

Supplementary materials

Supplementary material associated with this article can be found, in the online version, at doi:10.1016/j.addlet.2024.100250.

Data availability

Data will be made available on request.

References

[1] G.Z. Lum, Z. Ye, X. Dong, H. Marvi, O. Erin, W. Hu, M. Sitti, Shape-programmable magnetic soft matter, Proc. Natl. Acad. Sci 113 (2016) E6007–E6015.
[2] G. Liu, G.A.O. Fei, D. Wang, W.-H. Liao, Medical applications of magnetorheological fluid: a review, Smart Mater. Struct. (2022).
[3] V.Q. Nguyen, A.S. Ahmed, R.V. Ramanujan, Morphing soft magnetic composites, Adv. Mater. 24 (2012) 4041–4054, https://doi.org/10.1002/adma.201104994.
[4] K. Danas, S.V. Kankanala, N. Triantafyllidis, Experiments and modeling of iron-particle-filled magnetorheological elastomers, J. Mech. Phys. Solids 60 (2012) 120–138, https://doi.org/10.1016/j.jmps.2011.09.006.
[5] Y. Kim, G.A. Parada, S. Liu, X. Zhao, Ferromagnetic soft continuum robots, Sci. Robot. 4 (2019) eaax7329.
[6] A.V. Chertovich, G.V. Stepanov, E.Y. Kramarenko, A.R. Khokhlov, New composite elastomers with giant magnetic response, Macromol. Mater. Eng. 295 (2010) 336–341.
[7] Y. Kim, X. Zhao, Magnetic soft materials and robots, Chem. Rev. 122 (2022) 5317–5364, https://doi.org/10.1021/acs.chemrev.1c00481.
[8] A.K. Bastola, M. Hossain, The shape – morphing performance of magnetoactive soft materials performance, Mater. Des. 211 (2021) 110172, https://doi.org/10.1016/j.matdes.2021.110172.
[9] Y. Lu, D. Yu, H. Dong, J. Lv, L. Wang, H. Zhou, Z. Li, J. Liu, Z. He, Magnetically tightened form-stable phase change materials with modular assembly and geometric conformality features, Nat. Commun. 13 (2022) 1397, https://doi.org/10.1038/s41467-022-29090-1.
[10] U. Bozuyuk, O. Yasa, I.C. Yasa, H. Ceylan, S. Kizilel, M. Sitti, Light-triggered drug release from 3D-printed magnetic chitosan microswimmers, ACS Nano 12 (2018) 9617–9625.
[11] MAGNETS ADVANCED. Typical physical and chemical properties of some magnetic materials, 2007.
[12] O. Gutfleisch, M.A. Willard, E. Brück, C.H. Chen, S.G. Sankar, J.P. Liu, Magnetic materials and devices for the 21st century: stronger, lighter, and more energy efficient, Adv. Mater. 23 (2011) 821–842, https://doi.org/10.1002/adma.201002180.
[13] K. Genc, Processing of NdFeB for electric motor applications using selective laser melting, (2022).
[14] L. Miao, Y. Song, Z. Ren, C. Xu, J. Wan, H. Wang, H. Guo, Z. Xiang, M. Han, H. Zhang, 3D Temporary-magnetized soft robotic structures for enhanced energy harvesting, Adv. Mater. 33 (2021) 2102691, https://doi.org/10.1002/adma.202102691.
[15] Z. Ji, C. Yan, B. Yu, X. Wang, F. Zhou, Multimaterials 3D printing for free assembly manufacturing of magnetic driving soft actuator, Adv. Mater. Interfaces 4 (2017) 1–6, https://doi.org/10.1002/admi.201700629.
[16] C. Ma, S. Wu, Q. Ze, X. Kuang, R. Zhang, H.J. Qi, R. Zhao, Magnetic multimaterial printing for multimodal shape transformation with tunable properties and shiftable mechanical behaviors, ACS Appl. Mater. Interfaces 13 (2021) 12639–12648, https://doi.org/10.1021/acsami.0c13863.

[17] Y. Dong, L. Wang, N. Xia, Z. Yang, C. Zhang, C. Pan, D. Jin, J. Zhang, C. Majidi, L. Zhang, Untethered small-scale magnetic soft robot with programmable magnetization and integrated multifunctional modules, Sci. Adv. 8 (2022) eabn8932.
[18] O. Yasa, Y. Toshimitsu, M.Y. Michelis, L.S. Jones, M. Filippi, T. Buchner, R. K. Katzschmann, An overview of soft robotics, Annu. Rev. Control. Robot. Auton. Syst. 6 (2023) 1–29.
[19] S. Sundaram, M. Skouras, D.S. Kim, L. van den Heuvel, W. Matusik, Topology optimization and 3D printing of multimaterial magnetic actuators and displays, Sci. Adv. 5 (2019) eaaw1160.
[20] A.P. Taylor, C.V. Cuervo, D.P. Arnold, L.F. Velásquez-García, Fully 3D-printed, monolithic, mini magnetic actuators for low-cost, compact systems, J. Microelectromechanical Syst. 28 (2019) 481–493.
[21] E.B. Joyee, A. Szmelter, D. Eddington, Y. Pan, 3D printed biomimetic soft robot with multimodal locomotion and multifunctionality, Soft Robot 9 (2022) 1–13.
[22] R. Domingo-Roca, J.C. Jackson, J.F.C. Windmill, 3D-printing polymer-based permanent magnets, Mater. Des. 153 (2018) 120–128.
[23] Q. Lu, K. Choi, J.-D. Nam, H.J. Choi, Magnetic polymer composite particles: design and magnetorheology, Polym. 13 (2021), https://doi.org/10.3390/polym13040512.
[24] E.A. Périgo, J. Jacimovic, F. García Ferré, L.M. Scherf, Additive manufacturing of magnetic materials, Addit. Manuf. 30 (2019) 100870, https://doi.org/10.1016/j.addma.2019.100870.
[25] J. Wu, N.T. Aboulkhair, M. Degano, I. Ashcroft, R.J.M. Hague, Process-structure-property relationships in laser powder bed fusion of permanent magnetic Nd-Fe-B, Mater. Des. 209 (2021) 109992, https://doi.org/10.1016/j.matdes.2021.109992.
[26] K.-S. Yu, C.-W. Cheng, A.-C. Lee, W.-Y.Jhang Jian, W.-C. Chang, T.-W. Chang, M.-C. Tsai, Additive manufacturing of NdFeB magnets by synchronized three-beam laser powder bed fusion, Opt. Laser Technol. 146 (2022) 107604, https://doi.org/10.1016/j.optlastec.2021.107604.
[27] M.P. Paranthaman, N. Sridharan, F.A. List, S.S. Babu, R.R. Dehoff, S. Constantinides, Additive manufacturing of near-net shaped permanent magnets, Proj. Rep. Oak Ridge Natl. Lab. (2016).
[28] H. Wu, O. Wang, Y. Tian, M. Wang, B. Su, C. Yan, K. Zhou, Y. Shi, Selective laser sintering-based 4D printing of magnetism-responsive grippers, ACS Appl. Mater. Interfaces 13 (2021) 12679–12688, https://doi.org/10.1021/acsami.0c17429.
[29] M.P. Paranthaman, C.S. Shafer, A.M. Elliott, D.H. Siddel, M.A. McGuire, R. M. Springfield, J. Martin, R. Fredette, J. Ormerod, Binder jetting: a novel NdFeB bonded magnet fabrication process, Jom 68 (2016) 1978–1982.
[30] Y. Kim, H. Yuk, R. Zhao, S.A. Chester, X. Zhao, Printing ferromagnetic domains for untethered fast-transforming soft materials, Nature 558 (2018) 274–279.
[31] X. Cao, S. Xuan, S. Sun, Z. Xu, J. Li, X. Gong, 3D printing magnetic actuators for biomimetic applications, ACS Appl. Mater. Interfaces 13 (2021) 30127–30136, https://doi.org/10.1021/acsami.1c08252.
[32] A.K. Bastola, M. Paudel, L. Li, Development of hybrid magnetorheological elastomers by 3D printing, Polym. (United Kingdom) 149 (2018), https://doi.org/10.1016/j.polymer.2018.06.076.
[33] L. Brusa da Costa Linn, K. Danas, L. Bodelot, Towards 4D printing of very soft heterogeneous magnetoactive layers for morphing surface applications via liquid additive manufacturing, Polym 14 (2022), https://doi.org/10.3390/polym14091684.
[34] M.L. Lopez-Donaire, G. de Aranda-Izuzquiza, S. Garzon-Hernandez, J. Crespo-Miguel, M. Fernandez-de la Torre, D. Velasco, D. Garcia-Gonzalez, Computationally guided DIW technology to enable robust printing of inks with evolving rheological properties, Adv. Mater. Technol. 8 (2023) 2201707, https://doi.org/10.1002/admt.202201707.
[35] K.N. Al-Milaji, R.L. Hadimani, S. Gupta, V.K. Pecharsky, H. Zhao, Inkjet printing of magnetic particles toward anisotropic magnetic properties, Sci. Rep. 9 (2019) 16261, https://doi.org/10.1038/s41598-019-52699-0.
[36] E. Saleh, P. Woolliams, B. Clarke, A. Gregory, S. Greedy, C. Smartt, R. Wildman, I. Ashcroft, R. Hague, P. Dickens, C. Tuck, 3D inkjet-printed UV-curable inks for multi-functional electromagnetic applications, Addit. Manuf. 13 (2017) 143–148, https://doi.org/10.1016/j.addma.2016.10.002.
[37] H. Song, J. Spencer, A. Jander, J. Nielsen, J. Stasiak, V. Kasperchik, P. Dhagat, Inkjet printing of magnetic materials with aligned anisotropy, J. Appl. Phys. 115 (2014) 17E308, https://doi.org/10.1063/1.4863168.
[38] W.C. Liu, V.H.Y. Chou, R.P. Behera, H.Le Ferrand, Magnetically assisted drop-on-demand 3D printing of microstructured multimaterial composites, Nat. Commun. 13 (2022) 5015, https://doi.org/10.1038/s41467-022-32792-1.
[39] M.A. Bijarchi, M.B. Shafii, Experimental Investigation on the dynamics of on-demand ferrofluid drop formation under a pulse-width-modulated nonuniform magnetic field, Langmuir 36 (2020) 7724–7740, https://doi.org/10.1021/acs.langmuir.0c00097.
[40] Xaar, Ultra high viscosity technology, (2022).
[41] Quantica, High-performance, multi-material 3D printing, NovoJet™ C-7, 2022.
[42] L. Guan, J. Fan, X.Y. Chan, H.Le Ferrand, Continuous 3D printing of microstructured multifunctional materials, Addit. Manuf. 62 (2023) 103373, https://doi.org/10.1016/j.addma.2022.103373.
[43] S. Holland, C. Tuck, T. Foster, Fluid gels: a new feedstock for high viscosity jetting, Food Biophys 13 (2018) 175–185.
[44] H. Yang, Y. He, C. Tuck, R. Wildman, I. Ashcroft, P. Dickens, R. Hague, High viscosity jetting system for 3D reactive inkjet printing, in: 2013 Int. Solid Free. Fabr. Symp., University of Texas at Austin, 2013.
[45] J. Ledesma-Fernandez, C. Tuck, R. Hague, High viscosity jetting of conductive and dielectric pastes for printed electronics, in: 2014 Int. Solid Free. Fabr. Symp., University of Texas at Austin, 2015.